Thermal Conductivity of Doped Polysilicon Layers

Angela D. McConnell, Srinivasan Uma, *Member, IEEE,* and Kenneth E. Goodson, *Associate Member, IEEE*

***Abstract*—The thermal conductivities of doped polysilicon layers depend on grain size and on the concentration and type of dopant atoms. Previous studies showed that layer processing conditions strongly influence the thermal conductivity, but the effects of grain size and dopant concentration were not investigated in detail. The current study provides thermal conductivity measurements for low-pressure chemical-vapor deposition (LPCVD) polysilicon layers of thickness near 1 μm doped with boron and phosphorus at concentrations between 2.0×10^{18} cm^{-3} and 4.1×10^{19} cm^{-3} for temperatures from 20 K to 320 K. The data show strongly reduced thermal conductivity values at all temperatures compared to similarly doped single-crystal silicon layers, which indicates that grain boundary scattering dominates the thermal resistance. A thermal conductivity model based on the Boltzmann transport equation reveals that phonon transmission through the grains is high, which accounts for the large phonon mean free paths at low temperatures. Algebraic expressions relating thermal conductivity to grain size and dopant concentration are provided for room temperature. The present results are important for the design of MEMS devices in which heat transfer in polysilicon is important. [654]**

***Index Terms*—MEMS, polysilicon, thermal conductivity, thin films.**

I. Introduction

POLYCRYSTALLINE silicon is common in MEMS and integrated circuits (ICs). The performance and reliability of many microdevices, such as microscale thermometers, pressure sensors, gas flow detectors, and fluid valve actuators, are strongly influenced by heat conduction [1]. Heat transfer can also adversely affect the operation of IC interconnects and high-voltage and high-power transistors [2]. To design and operate such devices effectively, it is critical to quantify the thermal conductivities for thin films of polysilicon, which differ substantially from those of bulk silicon. Depending on the application, polysilicon is deposited and doped using different techniques, which affect the microstructure and thus the observed thermal conductivity of the resulting material. The thermal conductivities of polysilicon layers depend on the deposition process details [3], the grain size and shape, and the concentration and type of dopant atoms. While several researchers have reported thermal conductivity data for doped polysilicon [3]–[12], these data are difficult to compare because the impurity concentrations and grain sizes are not precisely known. At present, it is not possible to predict the thermal conductivity that will result from a given impurity concentration and microstructure.

The thermal conductivities of single-crystal silicon layers have been previously investigated [1], [13]–[15]. Asheghi *et al.* [1], [14] found that, at temperatures below 200 K, the thermal conductivities of intrinsic silicon layers of thicknesses ranging from 0.42 μm to 1.60 μm were significantly less than those of bulk silicon due to phonon scattering on the layer boundaries. Phonons are the energy quanta of lattice vibrational waves and are the main energy carriers in dielectric materials. Ju *et al.* [15] observed that the thermal conductivity of intrinsic silicon layers of thickness near 100 nm was reduced by up to 50% at room temperature. For phosphorus and boron-doped silicon layers with impurity concentrations higher than 1.0×10^{17} cm^{-3}, impurity scattering causes a further reduction in thermal conductivity compared to pure silicon layers, particularly at low temperatures [13]. Specifically, for layers of 3 μm thickness with phosphorus and boron concentrations of 1.0×10^{18} cm^{-3}, the conductivities at 20 K are reduced by factors of approximately two and four, respectively, with the difference resulting from the disparity in mass of the two impurity types.

In contrast to the case for single-crystal silicon, polysilicon films contain grain boundaries which strongly scatter phonons, reducing the thermal conductivity. Phonon scattering at grain boundaries is difficult to model, because the transmission probability for phonons through grain boundaries depends on the relative orientations of the bounding crystals and on the concentration of related defects near the boundary [16]. The thermal conductivity of undoped polysilicon layers has been measured from 20 K to 320 K [17] to isolate the effect of grain boundary scattering, which causes the largest thermal conductivity reduction at very low temperatures. This study included results for two layers, one of which was grown as polysilicon, while the other was deposited as amorphous silicon and subsequently annealed to allow recrystallization. The polysilicon grain size and shape varied significantly between these two layers. The observed thermal conductivities of both undoped polysilicon layers were one order of magnitude lower than those for undoped single-crystal silicon layers, but the amorphous recrystallized polysilicon layer had a higher thermal conductivity than the as-grown polysilicon due to larger grain sizes resulting from the high-temperature anneal.

Data for undoped polysilicon is of limited use in determining the thermal properties of doped polysilicon. Dopant atoms and their associated free electrons or holes contribute to phonon scattering [18], and the presence of dopants also affects the growth and size distribution of grains. N-type dopants, such

Manuscript received December 18, 2000; revised April 25, 2001. This work was supported in part by the National Science Foundation, the Stanford University School of Engineering and Department of Mechanical Engineering, and the Semiconductor Research Corporation under Contract 461. Subject Editor R. T. Howe.

A. D. McConnell and K. E. Goodson are with the Thermosciences Division of the Mechanical Engineering Department, Stanford University, Stanford, CA 94305 USA (e-mail: angela.mcconnell@stanford.edu; goodson@stanford.edu).

S. Uma was with the Thermosciences Division of the Mechanical Engineering Department, Stanford University. She is now with the Xerox-Palo Alto Research Center, Palo Alto, CA 94304 USA (e-mail: srinivas@parc.xerox.com).

Publisher Item Identifier S 1057-7157(01)05871-1.

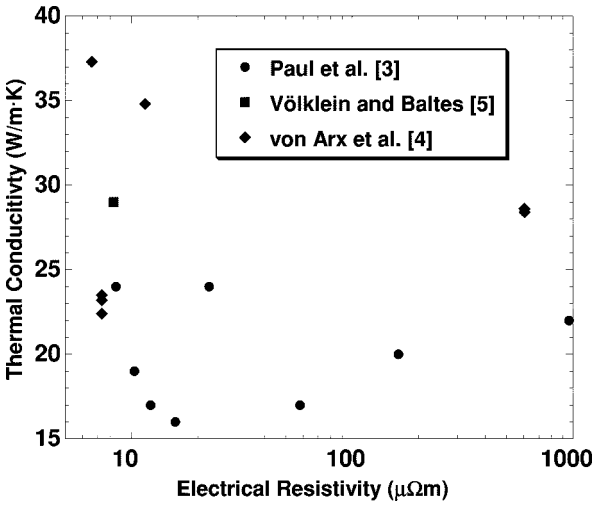

Fig. 1. Literature data for thermal conductivity (k) as a function of resistivity (ρ) for doped polysilicon layers. This figure excludes thermal conductivity data ranging between 29 and 35 W/m K for doped polysilicon film samples for which the resistivity was not reported [9]–[12].

as phosphorus, migrate to the grain boundaries in polysilicon, while p-type dopants, including boron, are uniformly distributed within the grains [19]. A high-temperature annealing process needed to activate the dopant atoms and repair damage to the crystal lattice after ion implantation promotes grain growth and also allows defects to diffuse out of the lattice.

The thermal conductivities of doped polysilicon layers have been measured in a few previous studies [3]–[12], and some of these results [3]–[5] are shown in Fig. 1 along with reported resistivity values. Much of this existing data has been collected for polysilicon in complementary metal–oxide–semiconductor (CMOS) layers [3]–[8], for which important parameters affecting the thermal conductivity, including the grain size, the dopant type and concentration, and the layer deposition temperature, are unavailable. In some cases the past work [3]–[5] estimated the carrier concentration through Hall effect measurements, but exact impurity concentrations cannot be determined from this information due to carrier trapping at the grain boundaries [20]. The lack of any apparent correlation between thermal conductivity and electrical resistivity data for the samples in Fig. 1 suggests that both grain size and impurity concentration varied among the samples. This illustrates the need for research on films in which these parameters are known, since this information is necessary to accurately model and predict the thermal conductivity of doped polysilicon layers.

The present work measures and predicts the influence of impurity type and concentration on the lateral thermal conductivities of four polysilicon layers at temperatures between 20 K and 320 K. The layers are approximately 1 μm thick and are doped with either boron or phosphorus at concentrations ranging from 2.0×10^{18} cm^{-3} to 4.1×10^{19} cm^{-3}. The measurements use Joule heating and electrical-resistance thermometry in a suspended membrane, an experimental structure closely resembling that used previously for doped single-crystal silicon films [13]. The thermal conductivity is modeled using the Boltzmann transport equation in the relaxation time approximation, which accounts for phonon scattering on grain boundaries, impurity atoms, and free electrons and holes.

This study aims to provide a resource for future thermal modeling work on MEMS and ICs. The layers are deposited using low-pressure chemical vapor deposition conditions typical for gate polysilicon in the IC industry and for conducting layers in micromachined sensors and actuators. The detailed modeling, which is verified using the data obtained here, is simplified to practical closed-form expressions relating the thermal conductivity to grain size and to impurity concentration and type. These simple models are perhaps the most important result of the current work, because they can be readily included in finite-element analysis and other computer-aided design (CAD) tools.

II. EXPERIMENTS

Several experimental methods are available for measuring the lateral thermal conductivities of thin films. These techniques generally use a suspended membrane containing the film, which is fabricated with etching processes. Electrical methods use Joule heating by sending electrical current through a bridge machined on the sample layer. Steady state electrical techniques have been applied extensively to polysilicon microcantilevers [3]–[5], [7], [8] and microbridges [10]–[12]. Optical methods include the transient thermal grating method, which uses laser heating and does not require contact with the sample [21]. While both electrical and optical techniques have been applied to films of thickness near 1 μm, electrical methods tend to provide lower experimental uncertainty because they facilitate precise, local heating. The current study adapts steady-state electrical heating in a suspended membrane.

A. Structure Fabrication and Characterization

Four doped polysilicon layers are prepared for the thermal conductivity measurements in this study. The layers are grown as polysilicon at a deposition temperature of 620 °C using low pressure chemical vapor deposition (LPCVD) in a Tylan furnace with a Silane (SiH_4) flow rate of 136 cm^3/min, a hydrogen flow rate of 110 cm^3/min, and a process pressure of 53.3 Pa [17]. A Nanospec Optical Spectrophotometer gives the layer thicknesses as 1.06 μm, which is accurate to $\pm$10%. Ion implantation is used to dope two of the layers with boron and two with phosphorus, and all four samples are subsequently annealed to homogeneously distribute the dopant atoms throughout the layer thickness and to electrically activate the dopants. A uniform doping profile is required to accurately characterize the effects of dopant atoms on thermal conductivity. Secondary ion mass spectroscopy (SIMS) measures the resulting dopant concentrations and confirms that the doping profiles are nearly homogeneous throughout the layer thickness. Table I gives the ion dose, implantation energy, annealing time and temperature, and resulting dopant concentration for each of the layers.

Transmission electron microscopy (TEM) characterizes the grain size of the doped polysilicon layers. The average grain size for each of the samples is estimated from plan-view TEM images contained in Fig. 2 using the line-intercept method. The

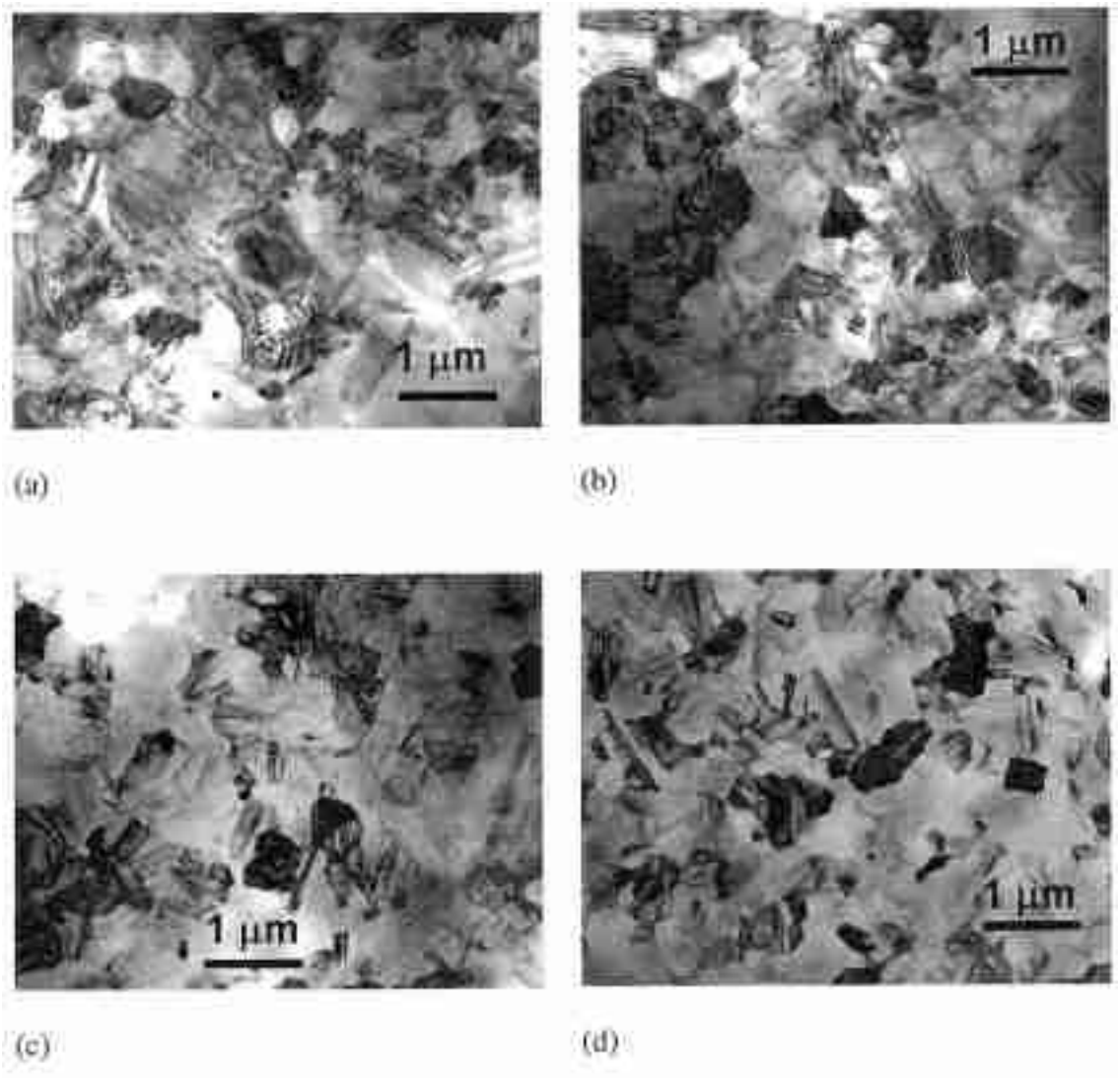

Fig. 2. Plan-view TEM images of the doped polysilicon layers, showing the grain sizes. (a) Sample 1, 2.0×10^{18} cm^{-3} B, $d_g = 400$ nm. (b) Sample 2, 1.6×10^{19} cm^{-3} B, $d_g = 408$ nm. (c) Sample 3, 2.4×10^{19} cm^{-3} P, $d_g = 313$ nm. (d) Sample 4, 4.1×10^{19} cm^{-3} P, $d_g = 295$ nm.

TABLE I
ION IMPLANTATION DETAILS FOR THE DOPED POLYSILICON LAYERS

Sample	1	2	3	4
Dopant	Boron	Boron	Phosphorus	Phosphorus
n [cm^{-3}]	2.0×10^{18}	1.6×10^{19}	2.4×10^{19}	4.1×10^{19}
Layer thickness [μm]	1.06	1.06	1.06	1.06
Dose [ions/cm^2]	3×10^{15}	2×10^{15}	3×10^{15}	5×10^{15}
Energy [KeV]	140	120	180	180
Anneal time [minutes]	80	40	60	40
Anneal temperature [°C]	1100	1100	1150	1100
Grain size [nm]	400	408	313	295

grain sizes range from 295 nm to 408 nm and are listed in Table I.

The free-standing structure shown in Fig. 3 measures the lateral thermal conductivities of the four samples. The structure is fabricated using deep reactive ion etching with a deposited silicon dioxide layer as the etch stop, and the aluminum metal bridges are patterned with lithography and chemical wet etching. The polyimide layer protects the aluminum bridges against chemical corrosion during processing and provides mechanical support for the membrane [17].

B. Thermal Conductivity Measurement Procedure

The measurements use electrical resistance thermometry and Joule heating in the aluminum bridges in Fig. 3. Current is passed through the center bridge, which serves both as a heater and thermometer, while the other aluminum bridge located

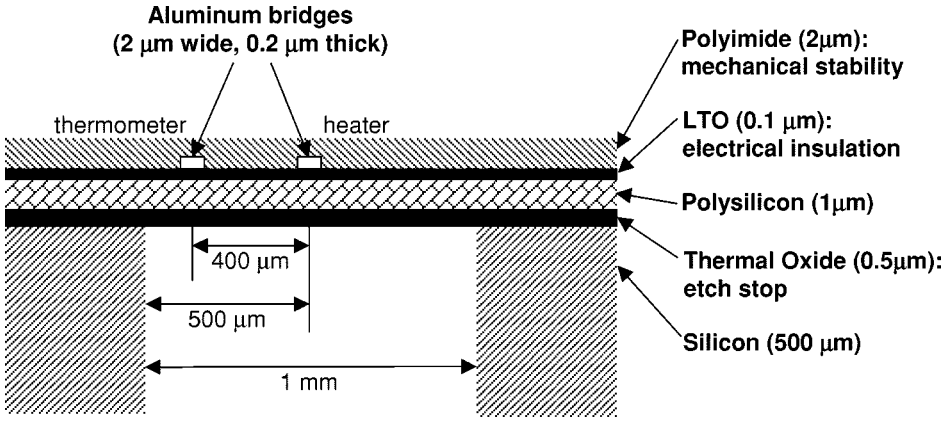

Fig. 3. Measurement structure schematic. The lateral and vertical dimensions are not in proportion.

400 μm from the center is used exclusively as a thermometer. The total length of the membrane is 13 mm, but only 1 mm at the center of the structure is used for the measurements to avoid two-dimensional effects. The sample is placed in a Lakeshore MTD-135 continuous flow cryostat, and measurements are taken at temperatures ranging from 20 K to 320 K, which are controlled using a diode sensor. The thermal conductivity experiments are performed in a vacuum to minimize the effects of convection.

The experimental structure is designed to ensure that lateral conduction through the polysilicon layer is the dominant mode of heat transport in the system. The thermal conductivity is calculated using the solution to the one-dimensional heat conduction equation

$$k = \frac{(Q/2) \cdot (X_{\text{thermometer}} - X_{\text{heater}})}{A_c \cdot (T_{\text{heater}} - T_{\text{thermometer}})}. \tag{1}$$

The temperatures T_{heater} and $T_{\text{thermometer}}$ are measured at the positions of the heater X_{heater} and the thermometer $X_{\text{thermometer}}$, and the cross-sectional area for heat conduction A_c is the product of the layer thickness and the heater line length. The heater power dissipated in the aluminum line Q is reduced by a factor of two, since the heater is located at the center of the free-standing layer.

C. Uncertainty Analysis

The uncertainty is dominated by contributions from the measured dimensions of the experimental structure shown in Fig. 3, in particular the polysilicon layer thickness. There is also a degree of uncertainty in the predicted heat losses from the structure through radiation and conduction along the silicon dioxide and polymer layers and in the measured voltages and currents. The uncertainty in both the structure dimensions and the measurements are considered using the sum-of-squares technique and the respective partial derivatives of (1) [21].

Heat generated in the aluminum heater lines can take several paths in addition to lateral conduction through the polysilicon layer. Heat is lost through conduction in the aluminum lines, radiation to the surroundings, and conduction in the other layers of the structure. Thermal contact resistance at the interface between the aluminum lines, oxide layer, and polysilicon layer also contributes some heat loss. The resistance of lateral conduction through the polysilicon layer is an order of magnitude or more smaller than these other modes of heat transfer, with radiation contributing the most error, particularly at room temperatures and above. To minimize the impact of radiation, the separation between the thermometers $X_{\text{heater}} - X_{\text{thermometer}}$ should be smaller than the thermal healing length of the layer due to radiation. The thermal healing length is based on conduction through an extended surface and is the characteristic length for the layer temperature to decay to the surrounding temperature T_0 [1]

$$L_H = \sqrt{\frac{d \cdot k}{\sigma \cdot (T^2 + T_0^2) \cdot (T + T_0)}} \tag{2}$$

where

- σ Stefan–Boltzmann constant;
- d polysilicon layer thickness;
- k polysilicon thermal conductivity;
- T average layer temperature.

At the highest measured temperatures for the sample with the lowest thermal conductivity in this study, the healing length is approximately 2.5 mm, which is much larger than the 400 μm separation between the heater and thermometer lines.

The total absolute uncertainty of the thermal conductivity is less than 15% throughout the range of measured temperatures. However, the uncertainty in the differences between the conductivities reported for the layers is much smaller, since the structure dimensions are nearly identical for all of the layers.

III. THERMAL CONDUCTIVITY MODELING

The local temperature-dependent thermal conductivities of the doped polysilicon layers are modeled by an approximate solution to the Boltzmann transport equation for phonons, which uses frequency-dependent relaxation times to represent phonon scattering events. Callaway [22] first developed this method, which Holland [23] later modified for silicon by considering phonon polarization. The current study extends the model of Holland [23] to account for the effects of grain boundaries and dopant atoms on the thermal conductivity.

The thermal conductivity of silicon is dominated by phonon conduction even for highly doped samples. Contributions from the mobile carriers (free holes or electrons) introduced by the dopant atoms in a semiconductor can increase its thermal conductivity. The electron contribution to the thermal conductivity

k_e at a given temperature T depends on the resistivity ρ and is calculated using the Wiedemann–Franz law

$$k_e = \frac{\pi^2 k_B^2}{3q^2} \cdot \frac{T}{\rho} \tag{3}$$

where q is the electron charge and k_B is the Boltzmann constant. Resistivity of a polysilicon layer is a function of dopant concentration [24], grain size [25], and doping technique [26]. The resistivities of the most heavily boron and phosphorus-doped layers in this study are estimated as 5×10^{-5} Ωm and 1.5×10^{-5} Ωm, respectively, based on values for single-crystal silicon [24]. The resistivity for polysilicon should be somewhat higher than for single-crystal silicon due to the grain boundaries, so these resistivity values correspond to an upper bound of the mobile carrier contribution to thermal conductivity. By (3), $k_e = 0.15\ \mathrm{W/m \cdot K}$ for the boron-doped layer and $0.46\ \mathrm{W/m \cdot K}$ for the phosphorus-doped layer at room temperature, which comprise only 0.3% and 0.8%, respectively, of the total observed thermal conductivity for these layers.

The thermal conductivity can be expected to vary with vertical position in the layers, owing to the variation in grain size. The experiments documented in this paper measure the thermal conductivity averaged in the z direction. The model developed here performs this average before comparison with the data.

A. Phonon Scattering in Bulk Silicon

Phonons from both the transverse (T) and longitudinal (L) branches of the phonon dispersion function contribute to the thermal conductivity k of a dielectric solid such as silicon [23]. The transverse mode is further divided into low-frequency (TO) and high-frequency (TU) ranges to account for dispersion

$$\begin{aligned} k &= \frac{1}{3} \sum_{j=L,TO,TU} v_j^2 \int_0^{\theta_j/T} C_{V,j} \tau_j \, dx_\omega \\ &= \frac{1}{3} \left(\frac{k_B T}{\hbar} \right)^3 \frac{k_B}{2\pi^2} \sum_{j=L,TO,TU} \frac{1}{v_j} \\ &\quad \cdot \int_0^{\theta_j/T} \frac{x_\omega^4 e^{x_\omega} \tau_j}{(e^{x_\omega} - 1)^2} \, dx_\omega. \end{aligned} \tag{4}$$

The phonon group velocity v_j varies for the different modes, with $v_{TO} = 5.86 \times 10^3$ m/s, $v_{TU} = 2.0 \times 10^3$ m/s, and $v_L = 8.48 \times 10^3$ m/s in silicon [23]. The dimensionless phonon angular frequency is defined as $x_\omega = \hbar\omega / k_B T$, where ω is the phonon angular frequency, T is the temperature, k_B is the Boltzmann constant, and $\hbar$ is Planck's constant divided by 2π. The relaxation times τ_j for the three modes consist of various phonon scattering events, which are combined using Matthiessen's rule

$$\tau_j^{-1} = \sum_i \tau_{j,i}^{-1}. \tag{5}$$

The temperatures θ_j in the integration limit of (4) correspond to the cutoff frequencies for the transverse and longitudinal modes. For silicon $\theta_{TO} = 180$ K, $\theta_{TU} = 210$ K, and $\theta_L = 570$ K [23].

The variation of thermal conductivity with temperature arises from the temperature dependence of the phonon scattering rates τ_j^{-1} and of the phonon specific heat, which contributes the low-temperature T^3 term in (4) [22]. Phonons scatter on other phonons in either normal (momentum-conserving) or Umklapp processes, on point defects and imperfections in the crystal lattice, and on specimen boundaries. The phonon–phonon Umklapp processes dominate the thermal resistance at room temperature and above, while defect and boundary scattering limit the thermal conductivity at low temperatures [27].

The thermal conductivity model for the doped polysilicon layers in the current study uses normal and Umklapp phonon–phonon scattering rates identical to those for bulk silicon given by Holland [23]. Normal scattering is significant only for the longitudinal and low-frequency transverse phonons, whereas Umklapp scattering contributes mainly in the high-frequency transverse mode.

Phonon scattering on point defects in the crystal lattice is treated as Rayleigh scattering, which assumes that the phonon wavelengths are much longer than the lattice spacing. This results in the following expression for the scattering rate,

$$\tau_{\mathrm{defect}}^{-1} = A\omega^4 \tag{6}$$

where ω is the phonon angular frequency and A is a constant related to the number of defects in the sample. Since the defect concentration in a layer depends on the deposition and processing conditions and cannot be readily obtained through experiments, the constant A is a fitting parameter.

Boundary scattering in a bulk specimen is most important at very low temperatures where the other scattering mechanisms are weak. At sufficiently low temperatures, the mean free path of an unlimited phonon would exceed the sample dimensions. Ziman [18] suggests a scattering rate for boundaries

$$\tau_{\mathrm{boundary}}^{-1} = \frac{v_s}{d} \left(\frac{1 - p(\omega)}{1 + p(\omega)} \right) \tag{7}$$

where d is the critical sample dimension, which is the polysilicon layer thickness in this study, and v_s is an averaged phonon group velocity

$$v_s^{-1} = \frac{1}{3} \left(\frac{2}{v_{TO}} + \frac{1}{v_L} \right). \tag{8}$$

The function $p(\omega)$ represents the probability of specular reflection from the sample boundary ($0 \le p \le 1$). A value of $p = 0$ corresponds to an entirely rough surface that diffusely scatters all incident phonons similar to a black body emitting absorbed radiation. Conversely, $p = 1$ designates a perfectly smooth surface which reflects all incoming phonons. Specularly reflected phonons can travel back and forth between the specimen walls before they are internally scattered by other processes, which is analogous to the flow of a rarefied gas in a tube. The probability of specular reflection p depends on the root-mean-squared (rms) surface roughness η and the phonon angular frequency ω [18],

$$p(\omega) = \exp\left[-\pi \left(\frac{2\eta\omega}{v_s} \right)^2 \right]. \tag{9}$$

Decreasing the phonon angular frequency increases the phonon wavelength relative to the surface roughness. The effective roughness of the surface then appears smaller to the phonons, so the probability of specular reflection increases.

B. Phonon Scattering on Grain Boundaries

Phonon scattering on grain boundaries in polycrystalline materials depends on the grain size and structure [16]. The grain structure in most polysilicon films deposited at temperatures between 600 °C and 650 °C is columnar with respect to the

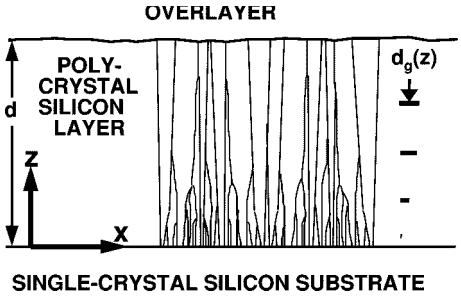

Fig. 4. Drawing of the columnar grain structure in polysilicon layers.

out-of-plane coordinate z [26], meaning the grains extend from the bottom surface of the layer to the top surface. The grain size for a columnar structure typically increases from the bottom of the layer to the top, as is illustrated schematically in Fig. 4. A linear approximation is assumed for the grain size in the present study

$$d_g(z) = (d_g(z=d) - d_g(z=0))\,\frac{z}{d} + d_g(z=0) \qquad (10)$$

where

z	coordinate perpendicular to the layer;
d	polysilicon layer thickness;
$d_g(z=d)$	maximum grain size;
$d_g(z=0)$	minimum grain size.

The maximum grain size is the average grain size obtained from the plan-view TEM images in Fig. 2, and the minimum grain size is estimated to be on the order of 100 nm for each of the layers. This relatively large value for the minimum grain size is expected to result from the very high annealing temperature.

The grain boundary scattering rate for lateral conduction in a layer with columnar grains can be approximated using (7)

$$\tau_{\text{grain}}^{-1} = \frac{v_s}{d_g(z)}\left(\frac{1-p_{tr}(\omega)}{1+p_{tr}(\omega)}\right). \qquad (11)$$

The grain size $d_g(z)$ is not necessarily the only critical parameter, because the probability of phonon reflection at a grain boundary can depend strongly on its roughness and on the density of related defects near the boundary. This complex situation can be modeled using $p_{tr}(\omega)$ as the probability of specular transmission $(0 \le p_{tr}(\omega) \le 1)$. Specular transmission at the grain boundaries increases the effective grain size. The parameter p_{tr} should decrease with decreasing phonon energy as the wavelength approaches the characteristic scales of boundary roughness and related defects. Therefore, the effective scattering strength of grain boundaries in a given film can be expected to increase with increasing temperature [28]. Assuming that the phonon specular transmission is dominated by grain boundary roughness, it can be approximated using (9) with η as the rms grain boundary roughness.

C. Phonon Scattering Due to Impurity Atoms

Dopant atoms in single-crystal silicon can significantly reduce the thermal conductivity, particularly at low temperatures [13], [29]. Some holes and electrons remain bound to the donor atoms, while others move freely in the valence band. Phonons can scatter on the impurities due to mass differences between the dopant and host (silicon) atoms and on the free and bound holes or electrons [18].

1) Boron (P-Type Dopants): P-type dopants are uniformly distributed within polysilicon grains, so they can therefore be modeled as additional point defect scattering sites in the crystal lattice. Impurity scattering exhibits the ω^4 dependence of Rayleigh scattering in (6) [18], with

$$A = \frac{nV^2}{4\pi v_s^3}\cdot\left(\frac{\Delta M}{M}\right)^2. \qquad (12)$$

The dopant concentration is denoted by n, V is the volume of the host (silicon) atom, v_s is the average phonon group velocity, M is the silicon atomic mass, and ΔM is the difference between the host (silicon) and impurity (boron) atomic masses.

2) Phosphorus (N-Type Dopants): In contrast to p-type dopants, a fraction of n-type dopants segregate to the grain boundaries in polysilicon. Depending on the dopant concentration and processing conditions, anywhere from approximately 25 to 75% of phosphorus atoms may segregate [19]. In addition to impurity scattering on the dopant atoms remaining within the grains as described by (12), the segregated dopant atoms alter the grain boundary scattering, which is modeled as follows [16]:

$$\tau_{\text{segragated dopants}}^{-1} = \frac{2v_s}{\pi d_g(z)} \cdot\left\{1+\left[\exp\left[\left(\frac{\pi}{2}\right)^2\cdot\zeta(\omega,z)\right]-1\right]^{-1}\right\}^{-1} \qquad (13)$$

where d_g is the grain size. The grain boundary scattering strength ζ, defined as

$$\zeta(\omega,z) = \sigma_s(\omega)\cdot N_{gb}(z) \qquad (14)$$

depends on the number of dopant atoms located at the grain boundaries so is a function of phonon angular frequency ω and vertical position z within the layer. The scattering cross-section σ_s for impurity atoms is given by

$$\sigma_s(\omega) = \frac{V^2\omega^4}{4\pi\, v_s^2} \qquad (15)$$

in which V is the atomic volume of silicon. The number density of defects N_{gb} is the dopant concentration n divided by the grain boundary area per unit volume B_V, which for columnar grains is approximately

$$B_V = \frac{\pi}{2d_g(z)}. \qquad (16)$$

It is difficult to estimate the fraction of segregated dopant atoms, so the model assumes that half of the phosphorus atoms are located near the grain boundaries and that the other half remain within the polysilicon grains.

3) Phonon Scattering on Free Electrons and Holes: Free electron and hole scattering is believed to be important in doped semiconductors in which the phonon mean free path is either independent of temperature or decreases with decreasing temperature and is much smaller than the size of the material. The combined effects of boundary and impurity scattering are usually not large enough to account for this behavior [30]–[32]. The thermal conductivity data collected for the doped polysilicon layers in the current study show phonon mean free paths that increase as the temperature decreases and that are larger than the average

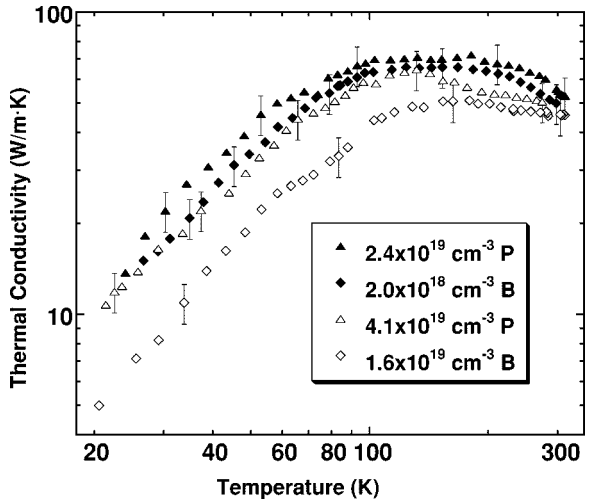

Fig. 5. Experimental data for the doped polysilicon layers.

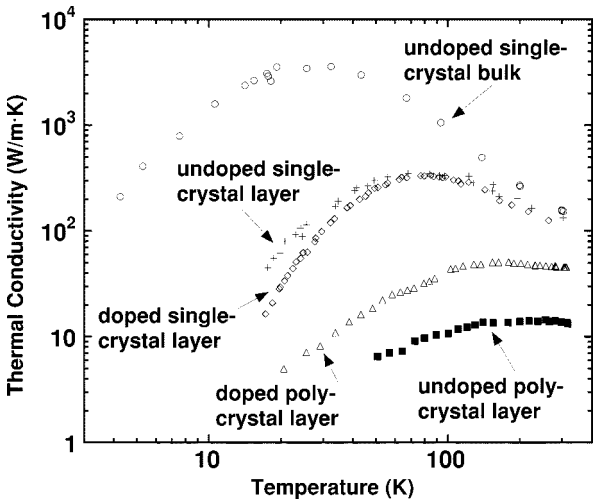

Fig. 6. Comparison of temperature-dependent thermal conductivity data for various silicon samples with the data from the present study. Undoped single-crystal bulk [35]: $d = 0.44$ cm. Undoped single-crystal layer [14]: $d = 1\ \mu$m. Doped single-crystal layer [13]: $d = 3\ \mu$m; $n = 1.0 \times 10^{19}$ cm^{-3} B. Doped poly-crystal layer: $d = 1\ \mu$m; $n = 1.6 \times 10^{19}$ cm^{-3} B; $d_g = 408$ nm. Undoped poly-crystal layer [17]: $d = 1\ \mu$m; $d_g = 190$ nm.

grain size at low temperatures, so phonon scattering on free carriers is not included in the thermal conductivity model. Phonon scattering on bound electrons and holes is also discussed in [33], but this mode of scattering becomes important only at very low temperatures (below 10 K) so is not considered in this study.

IV. Results and Discussion

A. Experimental Results

Fig. 5 shows that the thermal conductivity data for doped polysilicon are qualitatively consistent with the theory developed in Section III. For a given dopant type, the sample with the higher dopant concentration has lower thermal conductivity values since the larger number of impurities provides more scattering sites for the phonons. At a given dopant concentration, layers doped with phosphorus should have higher thermal conductivity values than boron-doped layers. Both layers doped with phosphorus do exhibit higher thermal conductivites at all temperatures than the layer doped with the highest boron concentration. This occurs because some of the phosphorus atoms collect at the grain boundaries in polysilicon, so there are fewer scattering sites for phonons in the phosphorus-doped layers compared to those doped with boron. Also, impurity scattering due to any phosphorus atoms remaining within the polysilicon grains is very small compared with that due to boron. From (6) and (12) the scattering rate of phonons on impurities is proportional to the square of the mass difference between silicon and the dopant atom. Since boron is much lighter than silicon while phosphorus and silicon have similar masses, the scattering rate for boron is nearly 36 times larger than for phosphorus.

The room-temperature thermal conductivities of the doped polysilicon layers in this study range from 45.6 W/m · K to 57.5 W/m · K, which are somewhat larger than the values shown in Fig. 1 for doped polysilicon layers in the literature. The highest thermal conductivity reported before the present work was 37.3 W/m · K [4] for a layer of thickness 275 nm, which is thinner than the layers of the present study with thickness 1 μm. The phonon mean free path is smaller in the thinner layer in part because of the increased scattering on layer boundaries. This effect is augmented by the fact that thinner layers need shorter anneal times to activate dopant atoms, such that smaller grain sizes are likely [34]. The carrier concentration measured for this layer is 2.4×10^{20} cm^{-3}, which means its dopant concentration must be significantly greater than any of the layers in this study. The combined effect of thinner layers, smaller grains, and more impurities is lower thermal conductivity values.

Fig. 6 shows the temperature-dependent thermal conductivity of the polysilicon layer doped with 1.6×10^{19} cm^{-3} boron along with measured thermal conductivity values reported by previous work. This qualitatively demonstrates the impact of phonon scattering on dopant atoms and on grain and layer boundaries. Compared to bulk single-crystal silicon, the maximum thermal conductivity value for the single-crystal silicon layer is an order of magnitude smaller and shifted to a higher temperature due to phonon scattering on the layer boundaries. The data of Asheghi *et al.* [13] indicate that doping single-crystal silicon layers with boron concentrations greater than 1.0×10^{17} cm^{-3} reduces the thermal conductivity only at temperatures below approximately 100 K. The room-temperature thermal conductivity approaches the same value for all three of these single-crystal silicon samples, which is consistent with the fact that boundary and impurity scattering are most important at lower temperatures. Fig. 6 reveals that the doped polysilicon layer has thermal conductivity values below those for the single-crystal layer doped with a comparable concentration at all temperatures. This implies that phonon scattering on grains of size $d_g = 408$ nm dominates the thermal resistance of a polysilicon layer with a boron concentration of approximately 10^{19} cm^{-3}.

The doped polysilicon layer exhibits higher thermal conductivity values at all temperatures than the undoped polysilicon layer shown in Fig. 6. These layers are grown under identical conditions, but the doped layer undergoes an annealing step to electrically activate the dopant atoms and repair lattice damage due to ion implantation. This high-temperature anneal also

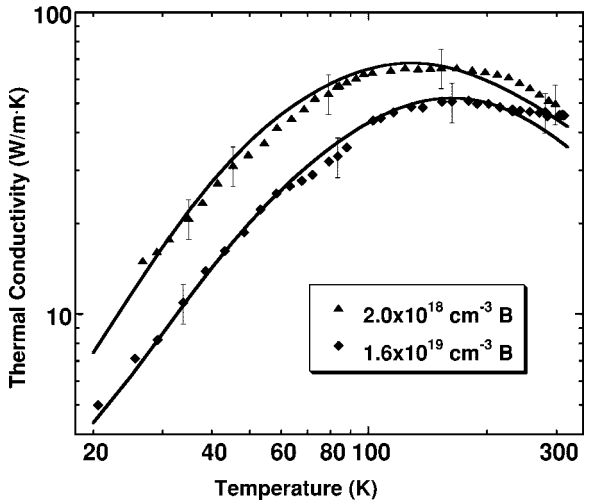

Fig. 7. Comparison of experimental data for the boron-doped polysilicon layers with the predictions of the modeling in Section III.

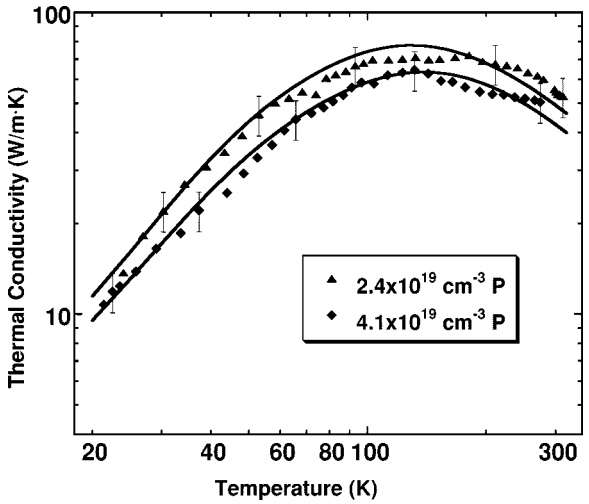

Fig. 8. Comparison of experimental data for the phosphorus-doped polysilicon layers with the predictions of the modeling in Section III.

causes grain growth, resulting in an average grain size of 408 nm for the doped layer compared to the 190 nm average grain size of the undoped layer [17]. Although the dopant atoms provide additional phonon scattering sites, the difference in grain sizes has a much greater impact on the observed thermal conductivity.

A previous study of bulk doped polysilicon (not shown in Fig. 6) reports a room-temperature thermal conductivity value of 40 W/m · K [29], which is surprisingly lower than the 45.6 W/m · K of the doped polysilicon layer. However, the bulk sample has a boron concentration of 5×10^{20} cm^{-3}, and neither its grain size nor structure was documented. This indicates that factors such as the microstructure or the increased number of impurities may have controlled the thermal conductivity of this bulk doped polysilicon specimen.

B. Modeling Results

Theoretical predictions of thermal conductivity are presented in Figs. 7 and 8 along with the experimental data for the two boron-doped and the two phosphorus-doped polysilicon layers, respectively. The theoretical model fits the measurements within the predicted error for all four layers throughout the entire investigated temperature range.

To implement the thermal conductivity model, parameters governing the doping, grain structure, layer geometry, and defect concentration are either obtained from known sample properties or chosen to best fit the experimental data. The only fitting parameters are the grain boundary roughness η_{grain} and the defect parameter A, which adjust the model at low and high temperatures, respectively. Table II lists the values of all parameters used in the model. The dopant type is known from processing, and the doping concentration n measured using SIMS varies among the samples. As described in Section III, approximately 25 to 75% of the phosphorus dopant atoms segregate to the grain boundaries in polysilicon [19]. Because it is difficult to estimate the fraction of segregated dopants, the model assumes that half of the phosphorus atoms are located near the grain boundaries and that the other half remain evenly distributed within the polysilicon grains. In the model, the choice of the segregated dopant fraction has the largest effect at room temperature. However, varying the fraction of segregated phosphorus atoms from 25 to 75% alters the resulting thermal conductivity by only 2.8%, so the predictions are consistent with the experimental data within the error bars. The average grain size at the top layer surface $d_g(z = d)$ obtained from the TEM images also varies for each sample, while the grain size at the bottom layer surface $d_g(z = 0)$ is set at a constant value for all samples. The rms grain boundary roughness η_{grain} should depend on the number of defects and impurities located at the grain boundaries. Since doping concentrations vary among the samples and each layer undergoes a different annealing process, the grain boundary roughness is a free parameter used to fit the model to the experimental data. The measured layer thickness d is constant for all of the layers since they are deposited in the same batch, and the rms layer roughness η_{layer} is given the same value for each layer. Finally, the defect scattering constant A from (6) depends on the defect concentration and is another free parameter.

The rms grain boundary roughness sizes needed to fit the experimental data lead to large values of phonon specular transmission through the grain boundaries at low temperatures. A high probability of specular transmission corresponds to phonon mean free paths that are longer than the average grain size. Although this may seem physically impossible, the experiments confirm this result. For samples 1, 2, 3, and 4, the phonon mean free path is larger than the average grain size at temperatures below approximately 36 K, 21 K, 47 K, and 42 K, respectively.

Fig. 9 illustrates the temperature-dependent contributions of the various phonon scattering mechanisms to the overall thermal resistance of the polysilicon layer doped with 1.6×10^{19} cm^{-3} boron. The curve with the lowest thermal resistance values results from using scattering rates for only the normal and Umklapp phonon processes. The thermal resistance increases with temperature because the phonon–phonon scattering rate is roughly proportional to the number of thermally-excited phonons, which increases as the temperature rises. At room temperature the thermal resistance approaches the inverse of

TABLE II
FITTING PARAMETERS USED TO OBTAIN AGREEMENT BETWEEN EXPERIMENTAL DATA AND MODELING RESULTS FOR THE DOPED POLYSILICON LAYERS

Sample	1	2	3	4
Dopant	Boron	Boron	Phosphorus	Phosphorus
n [cm^{-3}]	$2.0\text{x}10^{18}$	$1.6\text{x}10^{19}$	$2.4\text{x}10^{19}$	$4.1\text{x}10^{19}$
d_g (z=d) [nm]	400	408	313	295
d_g (z=0) [nm]	100	100	100	100
η_{grain} [nm]	0.1	0.35	0.1	0.135
d [μm]	1.1	1.1	1.1	1.1
η_{layer} [nm]	0.5	0.5	0.5	0.5
A [s^3]	$1.9\text{x}10^{-44}$	$1.0\text{x}10^{-44}$	$1.0\text{x}10^{-44}$	$1.0\text{x}10^{-44}$

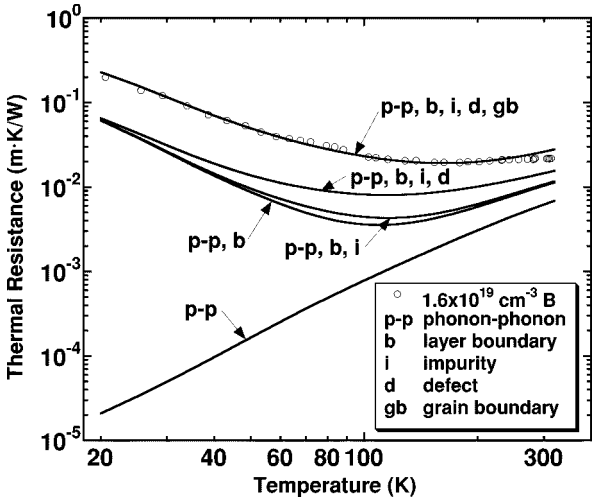

Fig. 9. Contributions of various phonon scattering mechanisms to the overall thermal resistance in polysilicon doped with 1.6×10^{19} cm^{-3} boron.

the thermal conductivity for bulk single-crystal silicon from Fig. 6. The next curve includes phonon scattering on the layer boundaries. The thermal resistance no longer decreases at the lowest temperatures because the layer thickness limits the phonon mean free path. Introducing impurity scattering slightly increases the thermal resistance at temperatures between approximately 40 K and 200 K, and defect scattering further increases the resistance at temperatures above 20 K. In contrast, grain boundary scattering leads to higher thermal resistance values at all temperatures. The experimental thermal conductivity data for the doped single-crystal silicon and the doped polysilicon layers in Fig. 6 confirm this observation.

C. Closed-Form Expression

The detailed thermal conductivity model is simplified to a closed-form expression relating the room-temperature thermal conductivity to grain size and to impurity concentration and type, all of which can be measured for a doped polysilicon layer. From the scattering rates given in Section III, the thermal conductivity is nearly proportional to the average grain size and inversely proportional to the dopant concentration. The thermal conductivity at 300 K is approximated by

$$k(d_g, n) = \frac{1}{3} C_S v_s \left(\frac{A_1}{d_g} + A_2 n \right)^{-1} \tag{17}$$

where $v_s = 6166$ m/s is the averaged phonon group velocity in silicon, $C_S = 1.654 \times 10^6$ J/m^{3}K is the phonon specific heat at 300 K in silicon, the average grain size d_g has units of nm, and the impurity concentration n has units of cm^{-3}. The constants in (17) are $A_1 = 2.887 \times 10^{10}$ and $A_2 = 3.200 \times 10^{-13}$ m^2 for boron-doped polysilicon, which fit the room-temperature data to within 5.5% and 0.6% for samples 1 and 2, respectively. For phosphorus-doped polysilicon, $A_1 = 2.887 \times 10^{10}$ and $A_2 = -1.122 \times 10^{-14}$ m^2, which fit the data for samples 3 and 4 to within 5.0% and 2.4%, respectively. The approximation of (17) is expected to be valid for all doping conentrations less than 3×10^{20} cm^{-3} and for grain sizes ranging from 100 nm to 1000 nm.

V. CONCLUSION

This study measures the temperature-dependent thermal conductivities of doped polysilicon layers with varying dopant types and concentrations. The thermal conductivities are significantly lower than those of single-crystal silicon layers across the entire investigated temperature range due to phonon scattering on the grain boundaries. At room temperature the thermal conductivity of a polysilicon layer is reduced by a factor of approximately two compared to a single-crystal silicon layer with a similar dopant concentration. The phonon mean free paths at temperatures below approximately 40 K are larger than the average grain size of the samples. A thermal conductivity model based on an approximate solution to the Boltzmann transport equation indicates that the transmission of phonons through the grain boundaries is high at low temperatures, which increases the effective grain size. Closed-form expressions that predict the thermal conductivity for doped polysilicon layers are developed which could be incorporated into simulations of practical devices using polysilicon.

REFERENCES

[1] M. Asheghi, Y. K. Leung, S. S. Wong, and K. E. Goodson, "Phonon-boundary scattering in thin silicon layers," *Appl. Phys. Lett.*, vol. 71, pp. 1798–1800, 1997.
[2] K. E. Goodson, "Thermal conduction in electronic microstructures," in *The CRC Handbook of Thermal Engineering*, F. Kreith, Ed. New York: CRC, 2000, pp. 4-458–4-504.
[3] O. Paul, M. von Arx, and H. Baltes, "Process-dependent thermophysical properties of CMOS IC thin films," in *Proc. 8th International Conference on Solid-State Sensors and Actuators, and Eurosensors IX*, Stockholm, Sweden, 1995.
[4] M. von Arx, O. Paul, and H. Baltes, "Process-dependent thin-film thermal conductivities for thermal CMOS MEMS," *J. Microelectromechan. Syst.*, vol. 9, pp. 136–145, 2000.
[5] F. Völklein and H. Baltes, "A microstructure for measurement of thermal conductivity of polysilicon thin films," *J. Microelectromechan. Syst.*, vol. 1, pp. 193–196, 1992.

[6] M. von Arx, O. Paul, and H. Baltes, "Determination of the heat capactiy of CMOS layers for optimal CMOS sensor design," *Sensors Actuators A*, vol. 46–47, pp. 428–431, 1995.
[7] O. M. Paul, J. Korvink, and H. Baltes, "Determination of the thermal conductivity of CMOS IC polysilicon," *Sensors Actuators A*, vol. 41–42, pp. 161–164, 1994.
[8] O. Paul and H. Baltes, "Thermal conductivity of CMOS materials for the optimization of microsensors," *J. Micromechan. Microeng.*, vol. 3, pp. 110–112, 1993.
[9] A. Irace and P. M. Sarro, "A novel technique to measure the thermal conductivity of thin film membranes," in *Proc. SPIE Conference on Materials and Device Characterization in Micromachining*, Santa Clara, CA, 1998.
[10] Y. C. Tai, C. H. Mastrangelo, and R. S. Muller, "Thermal conductivity of heavily doped low-pressure chemical vapor depositied polycrystalline silicon films," *J. Appl. Phys.*, vol. 63, pp. 1442–1447, 1988.
[11] C. H. Mastrangelo and R. S. Muller, "Thermal diffusivity of heavily doped low pressure chemical vapor depositied polycrystalline silicon films," *Sensors Mater.*, vol. 3, pp. 133–142, 1988.
[12] Y. C. Tai, C. H. Mastrangelo, and R. S. Muller, "Thermal conductivity of heavily doped LPCVD polysilicon," in *Proc. IEDM 87*, 1987.
[13] M. Asheghi, K. Kurabayashi, R. Kasnavi, J. Plummer, and K. E. Goodson, "Thermal conduction in doped single-crystal silicon films," in *Proc. 33rd National Heat Transfer Conference*, Albuquerque, NM, 1999.
[14] M. Asheghi, M. N. Touzelbaev, K. E. Goodson, Y. K. Leung, and S. S. Wong, "Temperature-dependent thermal conductivity of single-crystal silicon layers in SOI substrates," *J. Heat Transfer*, vol. 120, pp. 30–36, 1998.
[15] Y. S. Ju and K. E. Goodson, "Phonon scattering in silicon films with thickness of order 100 nm," *Appl. Phys. Lett.*, vol. 74, pp. 3005–3007, 1999.
[16] K. E. Goodson, "Thermal conduction in nonhomogeneous CVD diamond layers in electronic microstructures," *J. Heat Transfer*, vol. 118, pp. 279–286, 1996.
[17] S. Uma, A. D. McConnell, M. Asheghi, K. Kurabayashi, and K. E. Goodson, "Temperature dependent thermal conductivity of undoped polycrystalline silicon," *Int. J. Thermophys.*, vol. 22, pp. 605–616, 2001.
[18] J. M. Ziman, *Electrons and Phonons*. Oxford, U.K.: Oxford University Press, 1960.
[19] M. M. Mandurah, K. C. Saraswat, C. R. Helms, and T. I. Kamins, "Dopant segregation in polycrystalline silicon," *J. Appl. Phys.*, vol. 51, pp. 5755–5763, 1980.
[20] E. G. Lee and H. B. Im, "Effects of microstructure and As doping concentration on the electrical properties of LPCVD polysilicon," *J. Electrochem. Soc.*, vol. 138, pp. 3465–3469, 1991.
[21] K. E. Goodson, M. I. Flik, L. T. Su, and D. A. Antoniadis, "Prediction and measurement of the thermal conductivity of amorphous dielectric layers," *J. Heat Transfer*, vol. 116, pp. 317–324, 1994.
[22] J. Callaway, "Model for lattice thermal conductivity at low temperatures," *Physic. Rev.*, vol. 113, pp. 1046–1051, 1959.
[23] M. G. Holland, "Analysis of lattice thermal conductivity," *Physic. Rev.*, vol. 132, pp. 2461–2471, 1963.
[24] S. M. Sze, *Physics of Semiconductor Devices*, 2nd ed. New York: Wiley, 1981.
[25] N. C. C. Lu, L. Gerzberg, and J. D. Meindl, "A quantitative model of the effect of grain size on the resistivity of polycrystalline silicon resistors," *IEEE Electron Device Lett.*, vol. 1, pp. 38–41, 1980.
[26] S. M. Sze, *VLSI Technology*, 2nd ed. New York: McGraw-Hill, Inc., 1988.
[27] P. G. Klemens, "The thermal conductivity of dielectric solids at low temperatures," *Proc. Royal Soc. London*, ser. A, vol. 208, pp. 108–133, 1951.
[28] J. E. Graebner, M. E. Reiss, and L. Seibles, "Phonon scattering in chemical-vapor-deposited diamond," *Physic. Rev. B*, vol. 50, pp. 3702–3713, 1994.
[29] G. A. Slack, "Thermal conductivity of pure and impure silicon, silicon carbide, and diamond," *J. Appl. Phys.*, vol. 35, pp. 3460–3466, 1964.
[30] J. M. Ziman, "The effect of free electrons on lattice conduction," *Philosoph. Mag.*, vol. 1, pp. 191–198, 1956.
[31] ——, "The effect of free electrons on lattice conduction," *Philosoph. Mag.*, vol. 2, p. 292, 1957.
[32] G. P. Srivastava, *The Physics of Phonons*. Bristol, U.K.: Adam Hilger, 1990.
[33] K. Suzuki and N. Mikoshiba, "Effects of uniaxial stress and magnetic field on the low-temperature thermal conductivity of p-type Ge and Si," *J. Physic. Soc. Japan*, vol. 31, pp. 44–53, 1971.
[34] R. L. Bihan, F. Karray, and B. Cambou, "Grain size and resistivity of polycrystalline silicon films," in *Poly-Micro-Crystalline and Amourphous Semiconductors* Strasbourg, France, 1984.
[35] Y. S. Touloukian, R. W. Powell, C. Y. Ho, and P. G. Klemens, "Thermal conductivity of metallic elements and alloys," in *Thermophysical Properties of Matter*. New York: IFI/Plenum, 1970, vol. 1, pp. 326–339.

Angela D. McConnell received the Bachelor of Science degree in mechanical engineering with highest honors from the University of Illinois at Urbana-Champaign, in 1998. She then studied at Cambridge University, Cambridge, U.K., under a Churchill Scholarship and received the M.Phil. degree in engineering in 1999. She is currently pursuing the Ph.D. degree at Stanford University, Stanford, CA, where her studies are supported by a National Science Foundation graduate fellowship.

Her research interests include the thermal properties of thin-film materials and heat conduction in micro- and nanoscale structures.

Srinivasan Uma (M'00) received the Ph.D. degree in physics from the Indian Institute of Technology, Madras, India, in 1998.

She was a Guest Scientist at the Max-Planck-Institute for Solid-State Research, Stuttgart, Germany from 1995 to 1998 and carried out part of her Ph.D. research work with support from a German Academic Exchange Service Fellowship and a Max-Planck Institut Fellowship. From 1998 to 2000, she was a Postdoctoral Research Associate at the Mechanical Engineering Department, Stanford University, CA. Presently, she is working as an Experimental Physicist at the Xerox-Palo Alto Research Center, CA. Her current research interests include material science, thin film deposition and characterization, microscale heat transfer, and microelectromechanical systems.

Kenneth E. Goodson (M'95–A'96) received Bachelor's degrees in mechanical engineering and humanities from Massachusetts Institute of Technology (MIT), Cambridge, along with the Sudler Prize in 1989. He received the M.S. and Ph.D. degrees in mechanical engineering from MIT in 1991 and 1993, respectively, with a dissertation on self-heating of silicon-on-insulator transistors.

He is an Associate Professor of Mechanical Engineering at Stanford University, Stanford, CA. Before joining Stanford University in 1994, he worked with the Materials Research Group at Daimler-Benz AG on the thermal design of power circuits for vehicles. His Stanford University's research group, which includes 15 students and postdoctoral scholars, studies heat transfer in electronic systems with a focus on microscale conduction in novel thin films, transistors, and interconnect systems. In addition, he leads a multi-investigator DARPA/Intel/Stanford University effort on two-phase microchannel cooling for computers. He is coauthor of 80 archival journal articles and conference papers and four book chapters. In spring 1996, he was a JSPS Visiting Professor at the Tokyo Institute of Technology.

Dr. Goodson is a recipient of the ONR Young Investigator Award in 1996, the NSF CAREER Award in 1996, and the Outstanding Reviewer Award from the ASME Journal of Heat Transfer in 1999.